

Video Article

Cryosectioning Method for Microdissection of Murine Colonic Mucosa

Attila E. Farkas¹, Christian Gerner-Smidt¹, Loukia Lili¹, Asma Nusrat¹, Christopher T. Capaldo¹¹Epithelial Pathobiology and Mucosal Inflammation Research Unit, Department of Pathology and Laboratory Medicine, Emory University, Atlanta, GeorgiaCorrespondence to: Christopher T. Capaldo at ccapald@emory.eduURL: <https://www.jove.com/video/53112>DOI: [doi:10.3791/53112](https://doi.org/10.3791/53112)

Keywords: Cellular Biology, Issue 101, epithelia, mucosa, colon, crypt, microdissection, microtome

Date Published: 7/12/2015

Citation: Farkas, A.E., Gerner-Smidt, C., Lili, L., Nusrat, A., Capaldo, C.T. Cryosectioning Method for Microdissection of Murine Colonic Mucosa. *J. Vis. Exp.* (101), e53112, doi:10.3791/53112 (2015).

Abstract

The colonic mucosal tissue provides a vital barrier to luminal antigens. This barrier is composed of a monolayer of simple columnar epithelial cells. The colonic epithelium is dynamically turned over and epithelial cells are generated in the stem cell containing crypts of Lieberkühn. Progenitor cells produced in the crypt-bases migrate toward the luminal surface, undergoing a process of cellular differentiation before being shed into the gut lumen. In order to study these processes at the molecular level, we have developed a simple method for the microdissection of two spatially distinct regions of the colonic mucosa; the proliferative crypt zone, and the differentiated surface epithelial cells. Our objective is to isolate specific crypt and surface epithelial cell populations from mouse colonic mucosa for the isolation of RNA and protein.

Video Link

The video component of this article can be found at <https://www.jove.com/video/53112/>

Introduction

The colonic epithelial lining is a highly regenerative tissue, with resident stem cells replenishing the tissue every few days¹. This process of regeneration requires the maintenance of a proliferative stem cell compartment. Over time, the newly produced daughter cells lose their proliferative potential and migrate toward the luminal surface of the intestine. Coincident with migration, progenitor cells differentiate into mature barrier-forming enterocytes or mucous producing goblet cells. Failure of this differentiation program is thought to contribute to compromised epithelial barrier such as is observed in inflammatory bowel disease and colon cancer^{2,3}.

Detailed study of the above processes will require methodologies for isolating crypt-base and surface cell populations. Multiple methods exist, each with unique advantages and drawbacks. Current methods for the isolation of intestinal epithelial cells include chelating agents and mechanical disassociation, resulting in the isolation of entire crypts, epithelial sheets, or single cells, dependent on experimental conditions^{4,5}. These are high yield methods, yet changes in intercellular signaling have been reported under these conditions that may not represent the native environment^{6,7}. Laser capture microdissection allows for the collection of spatially distinct material, but achieves low molecular yield^{8,9}. In human colonic tissue, serial horizontal cryosectioning methods have been developed¹⁰. However, murine mucosal tissues are prohibitively small for direct appropriation of this technique. In humans, intestinal crypt lengths (the distance between the crypt-base and surface cells) in the colon varies between ~100–1,000 μm ¹¹. In mice, crypt lengths are between ~50–300 μm (see **Figure 1A**). The small size of murine crypts presents a challenge to the isolation of these two cell populations using existing protocols.

We now describe a low cost, high yield method for the isolation of crypt-base and surface epithelial cell population in murine colonic tissue. Tissue harvested in this manner may then be analyzed by a number of standard downstream applications, including immunofluorescence staining, RT-PCR (Real Time-Polymerase Chain Reaction) or western blotting.

Protocol

Experiments used C57BL/6 mice between 10 and 12 weeks of age. All procedures using animals were reviewed and approved by the Emory University Institutional Animal Care and Use Committee and were performed according to National Institutes of Health criteria.

1. Experimental Setup

1. Set Up the Cryostat
 1. Equilibrate cryostat to $-20\text{ }^{\circ}\text{C}$, including the microtome blade and chucks (exercise extreme caution around the blade!).
 2. Fill an empty cryomold with OCT (Optimal Cutting Temperature compound) and equilibrate to $-20\text{ }^{\circ}\text{C}$ (~30 min). Remove the frozen OCT from the mold and fix it on the chuck with liquid OCT. Place the block/chuck in the microtome arm and allow the OCT to set for 10 min.

3. Set the cryostat to 10 μm per section and shave the OCT block until it is flat. Back the microtome arm away from the blade by several centimeters. At this point do not adjust the blade or chuck for the remainder of the experiment.
2. Prepare the razor blades: Prepare 2 razor blades per sample. Using a metal file, dull the sharpened edge of blades. Next, remove the aluminum flange with forceps.
3. Pre-chill a Pyrex dish or other flat surface on dry ice.
4. Prepare a dissection dish with 10-15 dissection pins. A 10 cm tissue culture dish 50% filled with silicon will suffice. Add 5 ml of Hanks buffer at RT.

2. Dissection of Distal Colonic Tissue

1. Place mice in a sealed chamber and euthanize mice by isoflurane inhalation and cervical dislocation, then spray 70% ethanol onto the abdomen and thorax¹².
2. Make a small incision in skin of the abdomen with scissors and then make an incision to expose the peritoneal cavity. Similar procedures can be found described here¹².
3. Cut the large intestine at the anal verge and tease apart the mesentery until the colon is free.
4. Excise a distal colon segment between 0 and 6 cm from the anus. Here, the crypt depth is $\sim 150 \mu\text{m}$ (see **Figure 1B**). Cut open the colon longitudinally using scissors and remove the fecal contents.
5. Pin the tissue to the dissection dish with the mucosal surface facing up. Stretch the tissue using dissection pins on a silicon dish in Hanks buffer and let rest for 10 min at RT (**Figure 1C**). This removes folds from the tissue and allows the muscle layers to relax.

3. Mount Tissue on the Cryostat for Sectioning

1. Slide a razor blade under the desired section of tissue and then pour off the Hanks buffer. Add another razor blade to the top, making a sandwich. Cut the tissue segment and remove the pins. Transfer the razor blade/tissue sandwich to dry ice. Allow the tissue to freeze (5-10 min, **Figure 1D**).
2. Pick up the razor/tissue sandwich and allow it to warm slightly by placing a finger on the top blade (mucosal side up. This orients the tissue so that the basal muscle layers are sectioned first.). Separate the sandwich and cut around the edges of the tissue segment. Cut a tissue segment approximately, 0.5 cm x 1 cm. Edge areas have a tendency to curl, causing the serial sections to contain many tissue layers. Note that over-cutting is better than under-cutting, so err on the side of caution.
3. Allow the tissue to warm until the ice on top of the tissue begins to melt. At this point quickly and carefully press the tissue into the OCT block in the cryostat.
4. Remove the blade by placing a finger over the sample. The heat transfer will allow you to remove the blade without disrupting the tissue.
5. Coat the tissue with OCT and equilibrate for 5 min. Cut sections at 10 μm (**Figure 1E, F**). Visually inspect the sections until the crypts are seen. Place sections in a 1.5 ml tubes or on slides.
6. For analysis of mRNA or protein, place the samples in tubes with 5 crypt-base, 5 transitional, and 5 surface sections per tube. For RNA collection add 1 ml commercial isolation reagent and incubate at RT for 10 min. Perform RNA purification according to manufacturer's instructions. Use 5-10 μg of total RNA for cDNA generation.
7. For protein purification, add 0.5 ml of cold RIPA lysis buffer (plus protease inhibitors) per 5 sections. Sonicate 3 times at a 70% cycle, on ice.
 1. Add samples to SDS PAGE loading buffer (Laemmli buffer) and incubate at 100 $^{\circ}\text{C}$ for 10 min. Subject samples to SDS PAGE and transfer, then block in 5% milk/PBS for 2 hr. Perform western blot analysis followed by incubation with KLF4 antibodies (1:500) O/N at 4 $^{\circ}\text{C}$.

Representative Results

Colonic tissue sections were processed for histological assessment and H&E staining¹³. A traditional cross-section view of the mucosa is seen in **Figure 2A**. Basal areas contain the muscularis externa, composed mainly of the circular muscularis. Proceeding toward the lumen, the muscularis mucosa is evident adjacent to the crypt-base epithelial cells, transitional cells are in the middle of the tissue, and finally, surface cell populations face the gut lumen. The serial sectioning method described here maintains an orientation such that the longitudinal and circular muscularis are encountered first (**Figure 2B**), followed by the muscularis mucosa (**Figure 2C**). Note the appearance of non-muscle interstitial cells in the top left of the image. For the downstream analysis described below, muscle sections are discarded. The subsequent sections contain epithelial cells and interstitial tissue (lamina propria), starting with the crypt-base cells (**Figure 2D**). Note the absence of a central lumen in most of the crypts, which appear darker due to the closely packed nuclei. These layers contain the proliferative compartment. The transitional cells appear as tightly packed glands with prominent central lumens (**Figure 2E**). Lastly, surface cell populations have an irregular structure, with areas of the epithelial monolayer viewed *en face* (**Figure 2F**).

Serial sections as described above may also be processed for immunofluorescence labeling and confocal microscopy (as described here¹⁴). **Figure 2G** shows isolated crypts fixed and permeabilized in 100% methanol and subsequently stained for nuclei (blue) and the cell-cell junction protein Zonula Occludens 1 (ZO-1, green). In the traditional sectioning orientation, crypt and surface cell can be viewed simultaneously (**Figure 2G**). Note that the ZO-1 junctional stain lines the lumen of the colonic crypt. This ZO-1 lining of the lumen can also be seen in serial sectioned samples of transitional cell populations, in the center of the circular glands (**Figure 2G**). Enhanced ZO-1 stain is seen in surface cell populations (**Figure 2I and J**).

Several differentiation factors are known to be expressed in a spatiotemporal fashion along the crypt-to-surface axis. This includes the transcription factor Kruppel-like factor 4 (KLF4), which is known to be enriched in surface cell populations. Using traditional sectioning methods, KLF4 is found in the nuclei of lumen facing surface cell populations (**Figure 2K**). We therefore speculated that KLF4 mRNA would be predominantly expressed in surface cell populations. To test this, serial sections were collected and grouped into surface, transitional, and crypt-

base samples. Subsequently, RNA was harvested using standard Trizol extraction, with an additional purification by RNeasy column and DNase treatment. RNA was collected from 5 pooled consecutive sections, which yielded between 5-10 μg of total RNA per sample. These samples were then subjected to semi-quantitative real time PCR for both KLF4 and a reference gene, TATA box binding protein 1 (TBP-1) (**Figure 2L**)¹⁴. As shown in **Figure 2L**, after normalization to TBP-1, surface cells were found to express up to 8 times the KLF4 mRNA that is expressed in crypt cells. Similarly, KLF4 protein levels were found to exhibit spatial regulation along the crypt-surface axis. Serial sections were pooled as described above and then incubated in lysis buffer for 20 min at 4 °C. This yielded between 200-250 μg of protein per sample. Samples were then subjected analysis by SDS-PAGE (**Figure 2M**)¹⁵. As shown in **Figure 2M**, KLF4 protein levels are dramatically higher in surface cell populations. The above findings demonstrate the ability of this protocol to isolate large amounts of surface and crypt epithelial cells from the murine colonic mucosa.

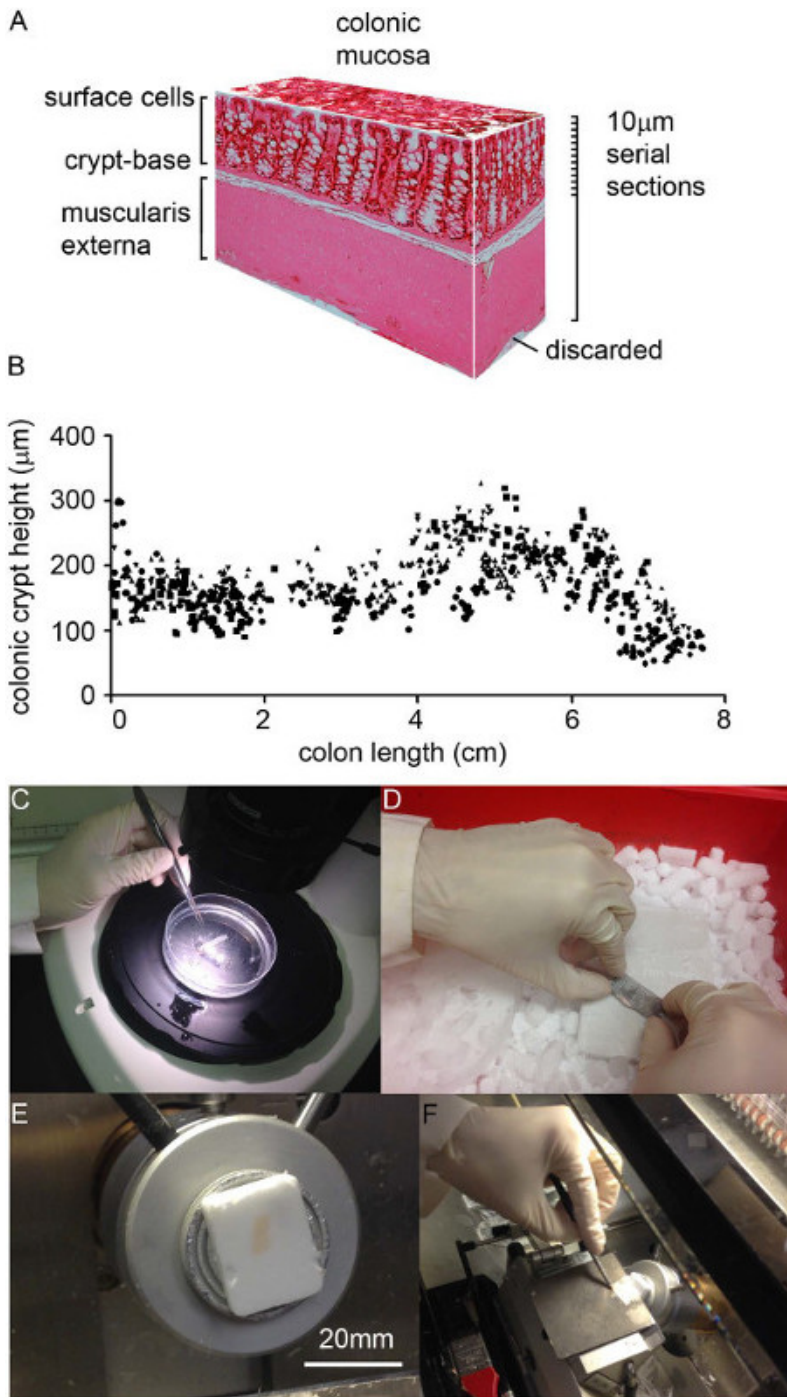


Figure 1: (A) Schematic showing murine colonic mucosa and external muscle layers. Our method aims to collect discrete surface cell and crypt-base cell populations by serial cryosectioning (10 μm each). The external muscle layers are discarded. (B) Crypt height varies along the length of the colon (distance between crypt-base and surface layers). Data points indicate individual crypt measurements and symbols indicate biological replicates (n = 4). (C) Colon segments collected, bisected, and pinned onto a silicon dissection dish. (D) A tissue segment approximately 3 cm from the anus is pressed between to razor blades and the frozen on dry ice. (E) Tissue is then mounted on a pre-leveled OCT block. (F) Cryosections are removed and visually inspected.

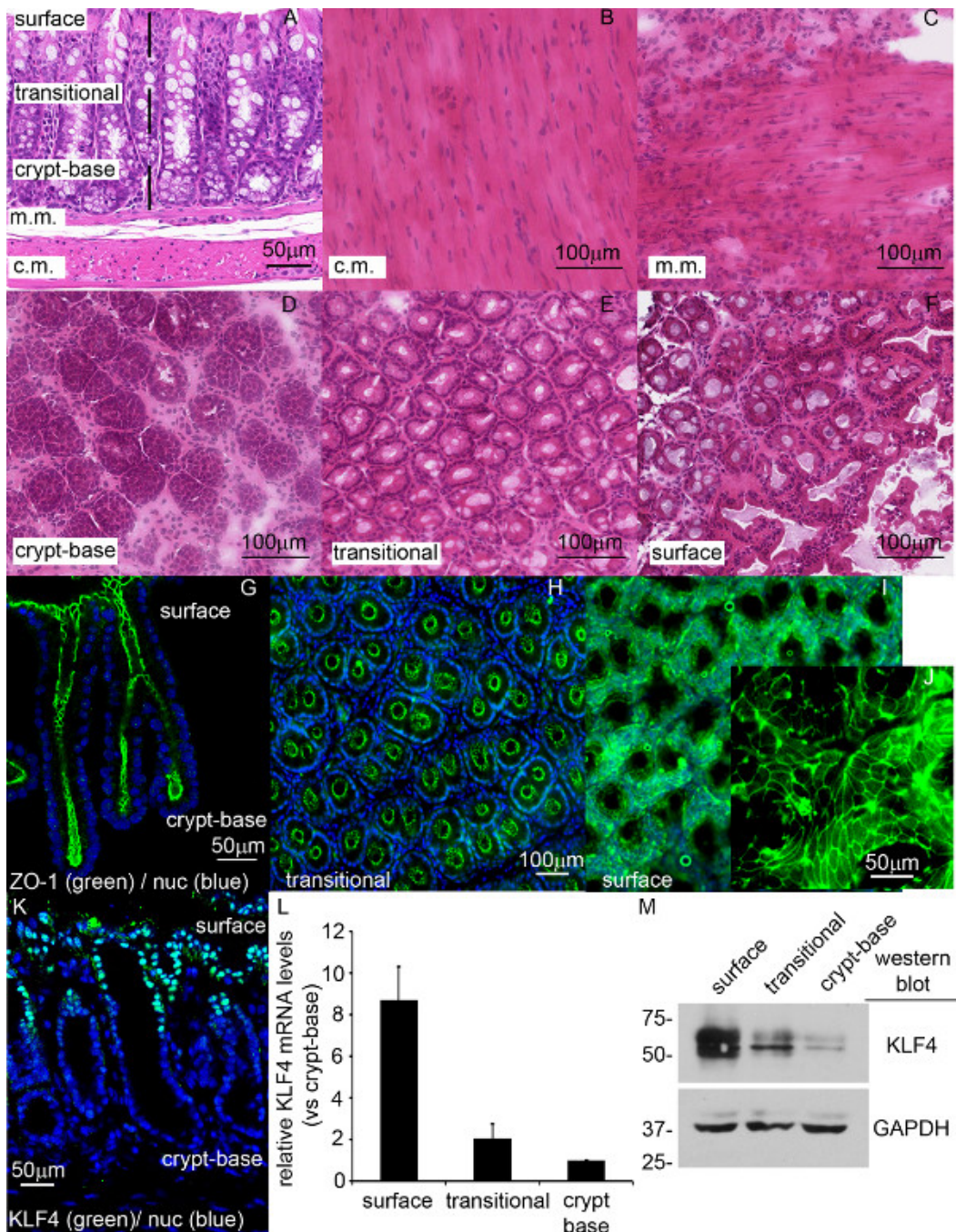


Figure 2: Representative data. (A) Colonic tissue stained with Hematoxylin-Eosin in cross-section showing the circular muscularis (c.m.), the muscularis mucosa (m.m.), crypt-base cells, transitional cells, and surface cells. (B-C) colonic muscle layers. (D) Crypt-base cells. Note the absence of a central lumen. (E) Transitional cells. (F) Surface cells. (G) Immunofluorescence staining of isolated colonic crypts. ZO-1 (green) and nuclei (blue) are observed in cross-section. (H-I) ZO-1 and nuclear staining in transitional and surface cells. (J) magnified view of ZO-1 staining. (K) KLF4 (green) is enriched in surface cell populations. (L) Real-time PCR assessment of KLF4 mRNA levels between the three compartments. (M) Western blot analysis of KLF4 protein levels in these cell populations.

Discussion

The molecular mechanisms involved in colonic epithelial cell proliferation and differentiation are poorly understood. This includes gaps in our understanding of the cellular signaling environment of the stem cell compartment at the base of the colonic epithelial crypts. There is also an increasing interest in the processes that underlie enterocyte differentiation. For example, increased understanding of *in vivo* differentiation is required as a benchmark for studies aimed at producing *in vitro* primary intestinal systems¹⁶.

The above procedure contains several steps that require extra attention. Firstly, removing the edges around the frozen tissue segment (as discussed in section 3.2) is required as the tissue edges curl during dissection and freezing. Failure to move these edges results in a mixed

population of surface and crypt base cells. Mounting the tissue on a pre-chilled, leveled OCT block is also essential. This protocol can be adapted to other areas of the distal colon by altering the number of sections in each pool. For example, as shown in **Figure 1B**, mucosal crypt length varies between 150-300 μm . Therefore, when studying the region between 4 cm-6 cm from the anus, the number of sections should be increased from 15 to 30. Importantly, this protocol is not suggested for the proximal colon (7 cm-9 cm) due to folds (plicae obliquae) which extend into the lumen making it impossible to separate surface and crypt-base cells by serial sectioning.

Serial sectioning techniques have been used to study crypt-base and surface epithelial cell populations in humans. However, our protocol adds additional steps that are required due to the small size of murine tissue. We propose that the above protocol will allow for the investigation of crypt-base and surface epithelial cell population in genetically tractable mouse systems. Indeed, pooled sections yield high quality protein and RNA suitable downstream analysis. Future applications could include the study of cell signaling pathways or chromatin immunoprecipitation. However, it should be noted that, like several of the alternative methods described above, the resulting sections contain a mixture of epithelial and interstitial lamina propria cells. In conclusion, the protocol described here provides a rapid, high yield method for the analysis of molecular processes in spatially distinct regions of the murine colonic mucosa.

Disclosures

The authors have nothing to disclose

Acknowledgements

Supported by National Institutes of Health (DK55679, and DK59888 to A.N.). Emory University Integrated Cellular Imaging Microscopy Core of the Winship Cancer Institute comprehensive cancer center grant, P30CA138292, and the Crohn's and Colitis Foundation of America Career Development award to C.T.C. and Fellowship Award to A.E.F.

References

- Noah, T. K., Donahue, B., Shroyer, N. F. Intestinal development and differentiation. *Exp Cell Res.* **317**, 2702-2710 (2011).
- Humphries, A., Wright, N. A. Colonic crypt organization and tumorigenesis. *Nat Rev Cancer.* **8**, 415-424 (2008).
- Weber, C. R., Turner, J. R. Inflammatory bowel disease: is it really just another break in the wall. *Gut.* **56**, 6-8 (2007).
- Bjerknes, M., Cheng, H. Methods for the isolation of intact epithelium from the mouse intestine. *Anat Rec.* **199**, 565-574 (1981).
- Sato, T., *et al.* Single Lgr5 stem cells build crypt-villus structures in vitro without a mesenchymal niche. *Nature.* **459**, 262-265 (2009).
- Rand, M. D., *et al.* Calcium depletion dissociates and activates heterodimeric notch receptors. *Mol Cell Biol.* **20**, 1825-1835 (2000).
- Gjorevski, N., Boghaert, E., Nelson, C. M. Regulation of Epithelial-Mesenchymal Transition by Transmission of Mechanical Stress through Epithelial Tissues. *Cancer Microenviron.* **5**, 29-38 (2012).
- Lechner, S., *et al.* Gene expression pattern of laser microdissected colonic crypts of adenomas with low grade dysplasia. *Gut.* **52**, 1148-1153 (2003).
- Reizel, Y., *et al.* Colon stem cell and crypt dynamics exposed by cell lineage reconstruction. *PLoS Genet.* **7**, e1002192 (2011).
- Kosinski, C., *et al.* Gene expression patterns of human colon tops and basal crypts and BMP antagonists as intestinal stem cell niche factors. *Proc Natl Acad Sci U S A.* **104**, 15418-15423 (2007).
- Tamura, S., *et al.* Pit pattern and three-dimensional configuration of isolated crypts from the patients with colorectal neoplasm. *J Gastroenterol.* **37**, 798-806 (2002).
- Geem, D., Medina-Contreras, O., Kim, W., Huang, C. S., Denning, T. L. Isolation and characterization of dendritic cells and macrophages from the mouse intestine. *Journal of visualized experiments : JoVE.* e4040 (2012).
- Laukoetter, M. G., *et al.* JAM-A regulates permeability and inflammation in the intestine in vivo. *J Exp Med.* **204**, 3067-3076 (2007).
- Neumann, P. A., *et al.* Gut commensal bacteria and regional Wnt gene expression in the proximal versus distal colon. *Am J Pathol.* **184**, 592-599 (2014).
- Capaldo, C. T., *et al.* Proinflammatory cytokine-induced tight junction remodeling through dynamic self-assembly of claudins. *Mol Biol Cell.* **25**, 2710-2719 (2014).
- Wells, J. M., Spence, J. R. How to make an intestine. *Development.* **141**, 752-760 (2014).